Case Analyses and Numerical Simulation of Soil Thermal Impacts on Land Surface Energy Budget Based on an Off-Line Land Surface Model

Guo Weidong (郭维栋)[1,2]†, Sun Shufen (孙菽芬)[2] and Qian Yongfu (钱永甫)[1]

[1]*Department of Atmospheric Sciences, Nanjing University, Nanjing* 210093

[2]*LASG, Institute of Atmospheric Physics, Chinese Academy of Sciences, Beijing* 100029

(Received April 5, 2001; revised January 31, 2002)

ABSTRACT

The statistical relationship between soil thermal anomaly and short-term climate change is presented based on a typical case study. Furthermore, possible physical mechanisms behind the relationship are revealed through using an off-line land surface model with a reasonable soil thermal forcing at the bottom of the soil layer.

In the first experiment, the given heat flux is 5 W m^{-2} at the bottom of the soil layer (in depth of 6.3 m) for 3 months, while only a positive ground temperature anomaly of 0.06°C can be found compared to the control run. The anomaly, however, could reach 0.65°C if the soil thermal conductivity was one order of magnitude larger. It could be even as large as 0.81°C assuming the heat flux at bottom is 10 W m^{-2}. Meanwhile, an increase of about 10 W m^{-2} was detected both for heat flux in soil and sensible heat on land surface, which is not neglectable to the short-term climate change. The results show that considerable response in land surface energy budget could be expected when the soil thermal forcing reaches a certain spatial-temporal scale. Therefore, land surface models should not ignore the upward heat flux from the bottom of the soil layer. Moreover, integration for a longer period of time and coupled land-atmosphere model are also necessary for the better understanding of this issue.

Key words: Soil thermal anomaly, Land surface model, Land surface energy budget

1. Introduction

Due to the enormous social and economic impacts of short-term climate change and its prediction, a series of Chinese national projects have been established (such as the Ninth-five-year Key Project of "Development of the Operational Prediction System for Short-term Climate Change" and the Key Project of the National Fundamental Research "Climate Dynamics and Prediction Theory").

Generally speaking, problems from both research and operation in this field can be classified as follows (Zhao 1998):

1) Some factors remain unknown. It is especially true as far as monthly-seasonal climate change predictions are concerned;

2) More importance should be attached to the significance and reliability of the factors which are currently widely used;

† E-mail: guowd@nju.edu.cn

3) A lot of signals are taken into consideration such as SST, snow cover, monsoon, subtropical high, blocking high, QBO, etc. But the relation and interaction among them have not been thoroughly studied yet.

The relationship between soil thermal anomaly and short-term climate change is a characteristic work conducted by Tang Maocang et al. for dozens of years. The study has been closely connected with the operational prediction since its very beginning in 1970s. Now it is one of the chief measures in China's flood / drought prediction due to its reliable performance. The main idea can be demonstrated by a conceptual model—' Geothermal Vortex' which illustrates the relation among earth interior thermal activity, soil temperature anomaly, underlying surface forcing and short-term climate (mainly precipitation) change (Tang et al. 1997a, b).

However, the physical mechanism explaining the influence of the soil temperature anomaly on precipitation remains not clear in spite of a lot of statistical results and operational applications. Insight studies are not available until recently thanks to the development of the sophisticated land surface model.

To acquire a specific impression on this issue, a typical case of severe floods in summer 1998 is reviewed before numerical study.

2. Case study

In July 1998, the distribution of soil temperature anomaly at the depth of 3.2 m (3.0 m in Taiwan) along with epicenters occurring in China within this period shows totally 16 regions with positive soil temperature anomaly (T'_s) (Fig. 1). While the contemporary distribution of

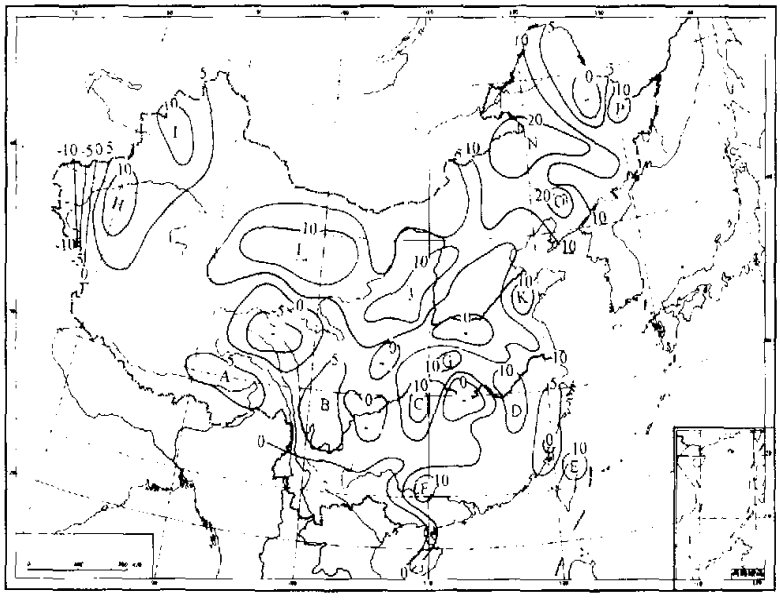

Fig. 1. Soil temperature anomaly at 3.2 m (3.0 m in Taiwan) over China in July 1998 (unit of the soil temperature anomaly is 0.1°C; A, B, C, ··· represents the positive anomaly region).

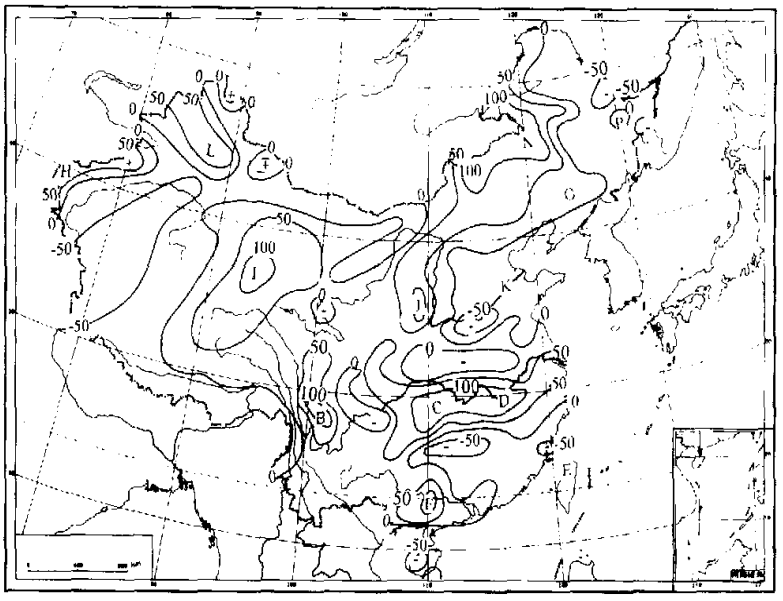

Fig. 2. Distribution of precipitation anomaly (R′%) over China in July 1998 (released by NCC) (A, B, C, ··· represents the center of rainy area corresponding to the positive soil temperature anomaly region).

precipitation anomaly (R′%) released by National Climate Center (NCC) indicates that two flood areas with R′% > 100% are located in mid–lower reaches of Yangtz River and central area of Inner Mongolia (i.e., Nenjiang River basin) respectively (Fig. 2). Most of the rainy / arid regions coincide well with positive / negative T'_s regions.

Guo (2000) has a detailed analyses on this case and pointed out that the above–mentioned regions with positive / negative soil temperature anomaly could be regarded as the reflections of the earth thermodynamic activities. The reason is that the seasonal fluctuation of ground temperature is almost removed from anomaly data and the soil temperature anomaly is mainly influenced by the heat flux from deeper soil layer.

This case analyses then present two challenges: (1) How to verify the existence and its behavior of the heat flux from deep soil layer? (2) The relationship between heat flux from deeper soil layer, soil temperature anomaly, and precipitation change. Since related studies are not available yet and the 1st question is critical to this paper, we should discuss it in detail as in section 3.2 and decide to choose an off–line land surface model. Sophisticated land surface model is a powerful tool to give a quantitative and step–by–step answer to the 2nd question. By doing so, we can lay emphases on the mechanism of soil thermal anomaly in influencing the soil temperature and land surface energy budget and lay a solid foundation for the following studies.

3. Numerical study

3.1 *Model description*

The numerical study is based on an off–line land surface model–NCAR LSM (Bonan

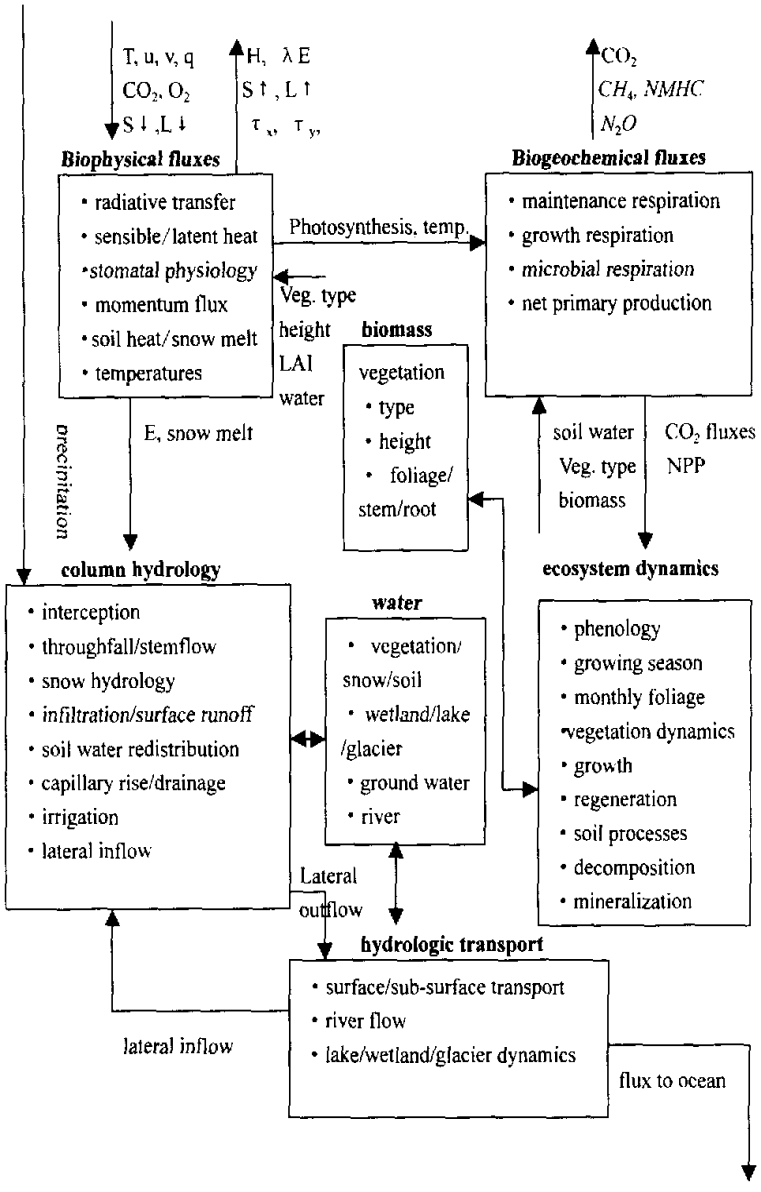

Fig. 3. Schematic diagram of model processes (the biophysical, biogeochemical, hydrologic, and ecosystem processes simulated by the model, interactions among these component processes, and the interaction between the land and atmosphere).

1995a, b; Bonan 1996). LSM is a one-dimensional model of energy, momentum, water, and CO_2 exchanges between the atmosphere and land accounting for ecological differences among vegetation types, thermal and hydrological differences among soil types, and multiple surface types, including lakes and wetlands, within a grid cell. The model is run for each subgrid point

independently, with the same grid-averaged atmospheric forcing. Grid-averaged surface variables are obtained using the subgrid fractional areas. Processes simulated for each subgrid points are: ecosystem dynamics, biophysical / hydrologic / biogeochemical processes (Fig. 3). The model is developed with the assumption that the land and atmosphere are coupled with a fully explicit time-stepping procedure.

The soil column is discretized into six layers with thickness of 0.10, 0.20, 0.40, 0.80, 1.60, and 3.20 m. Thermal properties (i.e., temperature, thermal conductivity, volumetric heat capacity) are defined at the center of each layer (Fig. 4).

For the purpose of our studies, more detailed explanations on sensible / latent heat flux calculation, soil / ground temperature update are presented in the following.

1) Sensible / latent heat fluxes

The sensible heat flux (H) and the latent heat flux (λE) between the atmosphere at reference height and the land are expressed by Bonan (1996)

$$H = -\rho_{\mathrm{atm}} c_p \frac{(\theta_{\mathrm{atm}} - \theta_s)}{r_{\mathrm{ah}}} , \tag{1}$$

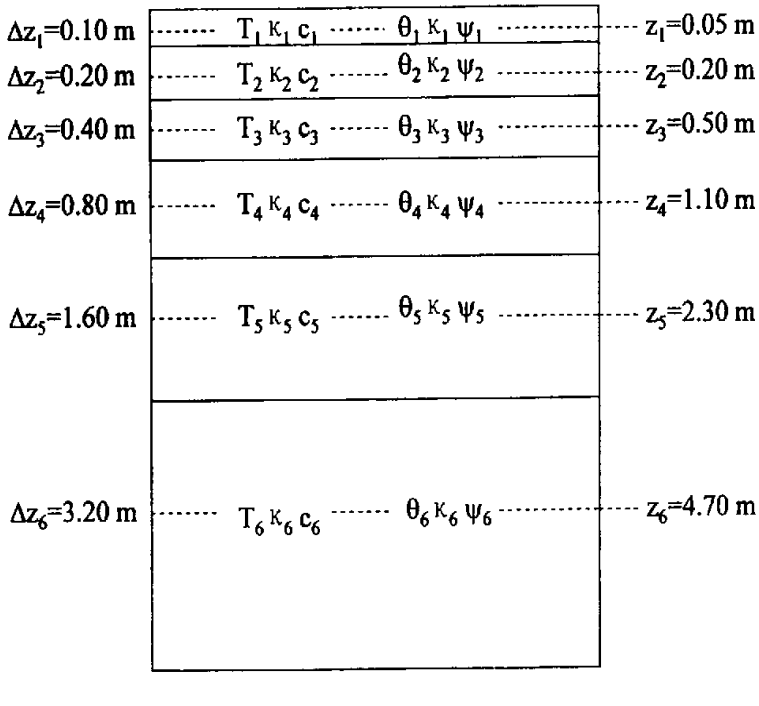

Fig. 4. Schematic diagram of the multi-layer soil profile. Thermal properties (temperature T_i, Thermal conductivity κ_i, volumetric heat capacity c_i) are defined at the center (depth z_i) of a layer with thichness Δz_i. The hydraulic properties (volumetric water content θ_i, hydraulic conductivity κ_i, and matrix potential ψ_i) are also defined at depth z_i

$$E = -\rho_{\mathrm{atm}} C_{\rho} \frac{(q_{\mathrm{atm}} - q_{\mathrm{s}})}{\gamma_{\mathrm{aeo}}} , \tag{2}$$

where ρ, θ, q, and γ are density, potential temperature, specific humidity and damping coefficient respectively. These formulas are derived by applying Monin–Obukhov similarity theory to the surface (i.e., constant flux) layer.

2) Ground temperature

The net long-wave radiation flux L, the sensible heat flux H, and the latent heat flux λE depend on the ground temperature T_{g}. With the soil heat flux G also a function of T_{g}, surface fluxes and temperatures are calculated by finding T_{g} that balances the energy budget:

$$-S_{\mathrm{g}} + L(T_{\mathrm{g}}) + H(T_{\mathrm{g}}) + \lambda E(T_{\mathrm{g}}) + G(T_{\mathrm{g}}) + M = 0 . \tag{3}$$

3) Soil temperature

With the heat flux F_z at depth z

$$F_z = -\kappa \frac{\partial T}{\partial z} , \tag{4}$$

one-dimensional energy conservation requires

$$\rho c \frac{\partial T}{\partial t} = -\frac{\partial F_z}{\partial z} = \frac{\partial}{\partial z}\left(\kappa \frac{\partial T}{\partial z}\right) , \tag{5}$$

where ρc is the volumetric soil heat capacity, T is the soil temperature and κ is the thermal conductivity. This equation is solved numerically to calculated soil temperatures for a six-layer soil with boundary conditions of G as the heat flux into the soil column and zero heat flux at the bottom of the soil column.

3.2 *Data and numerical scheme*

To drive the model, intensified atmospheric boundary layer data during GAME (GEWEX Asia Monsoon Experiment) / Tibet were utilized from June 16th to September 13th at an interval of 1 h. The field is Amdo in north Tibet Plateau at 32°14.5′N, 91°37.5′E. The data quality, determination of model parameters and the simulation ability of the model was evaluated by Zhang et al..①The conclusion is that the basic features of the land surface fluxes can be well reproduced by the model while sensible / latent heat fluxes and the surface reflected radiation are higher than the observed value.

As initial consideration: the ground temperature, the soil temperature from the 1st layer (5 cm in depth) to the 5th layer (at 230 cm) are set to the observed value as well as the soil moisture data. Vegetation temperature is set to air temperature, the leaf interception water is zero. The integration time step is 20 min while it is 10 min for soil temperature update. The radiation process is calculated every 1 h. And the atmospheric boundary layer data input to land model are read per hour.

---

①Zhang, Y., and S. H. Lu, Simulating the land surface processes in Amdo of Tibetan Plateau during summer monsoon season based on a land surface model (LSM). *Chinese Journal of Atmospheric Sciences*, (in press).

Table 1. List of some basic parameters in land surface model

Location	32°14.5′N, 91°37.5′E
Surface type	Cool grassland Cool grassland (0.6)
Vegetation type (proportion)	Warm grassland (0.2) Bare land (0.2) Sand (0.72)
Soil type (proportion)	Loam (0.20) Clay (0.08)
Soil color class	4

3.2.1 *On the intensity of heat flux into the bottom of the soil layer*

To guarantee the reliability of the sensitivity run, it is necessary to have a detailed discussion on the intensity of the soil thermal forcing before the experiment. Commonly, the heat conductivity equation is employed to describe the heat transfer in a multi-layer soil in current land surface models (Bonan 1996; Dickinson et al. 1993). To solve the equation, boundary conditions are required both on land surface and at the bottom of soil layer. The bottom boundary condition is usually set to zero, which means no ingoing / outgoing flux through the soil bottom.

However, what should be particularly pointed out is that the above mentioned condition may be improperly derived from the idea that the average observed ground heat flux is only 50 mW m^{-2}, which is too weak to take effects on short-term climate change. In fact, the underground heat flux should be the sum of conductive and convective components in which the observation is only the former(by multiplying soil temperature gradient with thermal conductivity). A case in point is that the ground heat flux at the center of the southeast Tibet "hot spot" can be as high as 25 W m^{-2} (Tang et al. 1998)! The value is larger than the mean by 500 times. The reason for such an incredible high value is that the convective heat flux is much greater than the conductive one in "hot spot" region due to the discharge of the hot fluids such as water vapor and CO_2 etc.

A detailed investigation on the release of the CO_2 in typical areas was proposed by Etiope and Klusman (1998). The discharge rate of CO_2 in active volcanic region is 38,400–146,000 t $km^{-2}yr^{-1}$. The amount in geothermal and tectonic region is less than the former but its maximum (in California) is 216,000 t $km^{-2}yr^{-1}$. The content of CO_2 in total geogases ranges from 10% to 95%. To estimate the heat flux associated with the surge of the hot fluid, we should identify the origin of the fluid. Up to now, only some geochemical analyses are available. The isotopic analyses in Southwest China show that the observed CO_2 consist of mixture both from the mantle and ground surface in which the mantle CO_2 takes at least 50% (Yuan 1999; Shangguan et al. 2000). Based on this result, taking the temperature in upper mantle (80 km in depth) as 800°C, the above mentioned maximum CO_2 flux reaches a heat flux of 5.5 W m^{-2}. And what is more, such significant CO_2 fluxes are also detected in China for times in faultage CO_2 observation (Lin①). This idea is applied to the determination of heat flux at the bottom of soil layer in the following numerical experiments.

①Lin, Y. W., Application of a convenient way in faultage CO_2 observation to earthquake prediction. (*to be published*)

3.2.2 *Experiment procedure*

First of all, the control run (CR) is conducted. The sensitive run (SR) is then carried out with a heat flux (determined by the discharge rate of CO_2) at the bottom of the soil layer. Taking both conductive and convective heat flux into account, 3 sets of sensitive run are accomplished with a forced heat flux of 5 W m^{-2} in the first set (SR1) and 10 W m^{-2} in SR3. The soil thermal conductive coefficient in SR2 and SR3 is one order of magnitude larger than that in SR1.

3.3 *Result analyses*

Similar evolution can be found in daily fluctuation of the ground soil heat flux, sensible heat and ground temperature of CR (Figs. 5a, b, c) since the ground temperature (T_g) is mainly decided by the net radiation and hydrologic state of the land and has direct influences on ground soil heat flux and sensible / latent heat flux.

Table 2. Differences between SR1 and CR (variables are 10-day averaged). (ΔF_{GE}, ΔF_{GR}, ΔF_{SH}, ΔT_g, ΔT_{s1} – ΔT_{s6} indicate the differences of ground evaporation, ground soil heat flux, sensible heat flux, ground temperature and soil temperature between SR1 and CR respectively. 01–10, ··· 81–93 are day numbers)

	ΔF_{GE} (W m^{-2})	ΔF_{GR} (W m^{-2})	ΔF_{SH} (W m^{-2})	ΔT_g (K)	ΔT_{S1} (K)	ΔT_{S2} (K)	ΔT_{S3} (K)	ΔT_{S4} (K)	ΔT_{S5} (K)	ΔT_{S6} (K)
01–10	0.00	0.00	0.00	0.00	0.00	0.00	0.00	0.00	0.02	0.44
11–20	0.00	−0.01	0.01	0.00	0.00	0.00	0.01	0.01	0.08	1.30
21–30	0.02	−0.04	0.02	0.00	0.00	0.01	0.02	0.04	0.18	2.13
31–40	0.02	−0.08	0.05	0.01	0.01	0.02	0.04	0.09	0.31	2.91
41–50	0.07	−0.16	0.07	0.01	0.01	0.03	0.08	0.15	0.48	3.65
51–60	0.13	−0.27	0.11	0.01	0.02	0.05	0.11	0.23	0.66	4.38
61–70	0.20	−0.39	0.14	0.02	0.03	0.06	0.14	0.30	0.84	5.09
71–80	0.25	−0.49	0.19	0.02	0.04	0.07	0.16	0.38	1.03	5.77
81–93	0.48	−0.93	0.32	0.06	0.08	0.13	0.23	0.48	1.26	6.51

Table 3. Same as Table 2 but the soil thermal conductivity (κ) in SR2 is greater than that in CR by one order of magnitude

	ΔF_{GE} (W m^{-2})	ΔF_{GR} (W m^{-2})	ΔF_{SH} (W m^{-2})	ΔT_g (K)	ΔT_{S1} (K)	ΔT_{S2} (K)	ΔT_{S3} (K)	ΔT_{S4} (K)	ΔT_{S5} (K)	ΔT_{S6} (K)
01–10	0.43	13.47	−11.5	−0.61	−0.46	−0.21	0.11	0.80	1.54	0.59
11–20	1.25	5.18	−5.16	−0.35	−0.14	0.16	0.46	1.09	2.91	2.03
21–30	0.55	−3.21	1.65	0.46	0.42	0.23	0.08	0.50	2.61	3.39
31–40	−0.74	1.56	−0.86	0.15	0.26	0.50	0.83	1.24	2.23	4.37
41–50	−1.11	0.59	0.32	0.07	0.14	0.41	0.80	1.32	2.45	5.15
51–60	0.38	−1.55	0.61	0.15	0.18	0.35	0.75	1.44	2.69	5.82
61–70	−0.85	0.51	−0.34	0.24	0.32	0.52	0.89	1.45	2.79	6.41
71–80	3.21	−6.64	2.72	0.30	0.29	0.26	0.47	1.34	3.02	6.91
81–93	0.50	−3.28	0.93	0.65	0.74	0.83	0.91	1.06	2.41	7.27

Since soil temperature (T_s) in control run mainly depends on the heat flux from land surface, the soil temperature profile features an adjustment toward the ground temperature

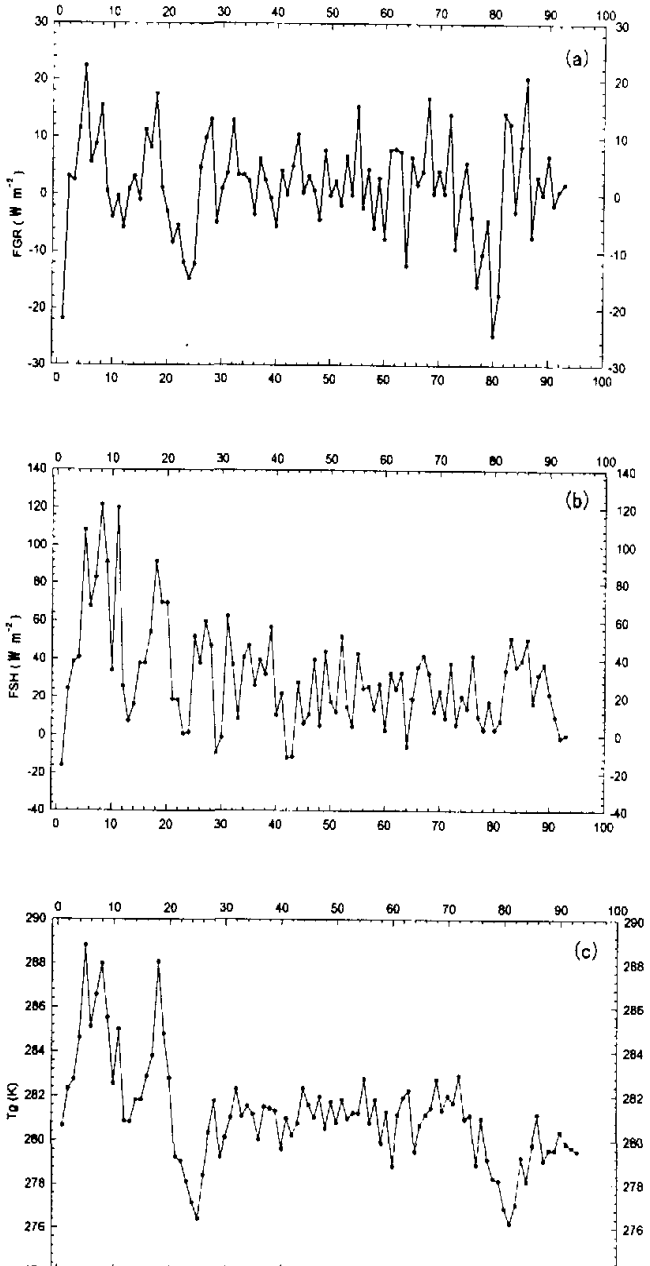

Fig. 5. Daily fluctuation of ground soil heat flux (a), sensible heat flux (b) and ground temperature (c) in control run (CR).

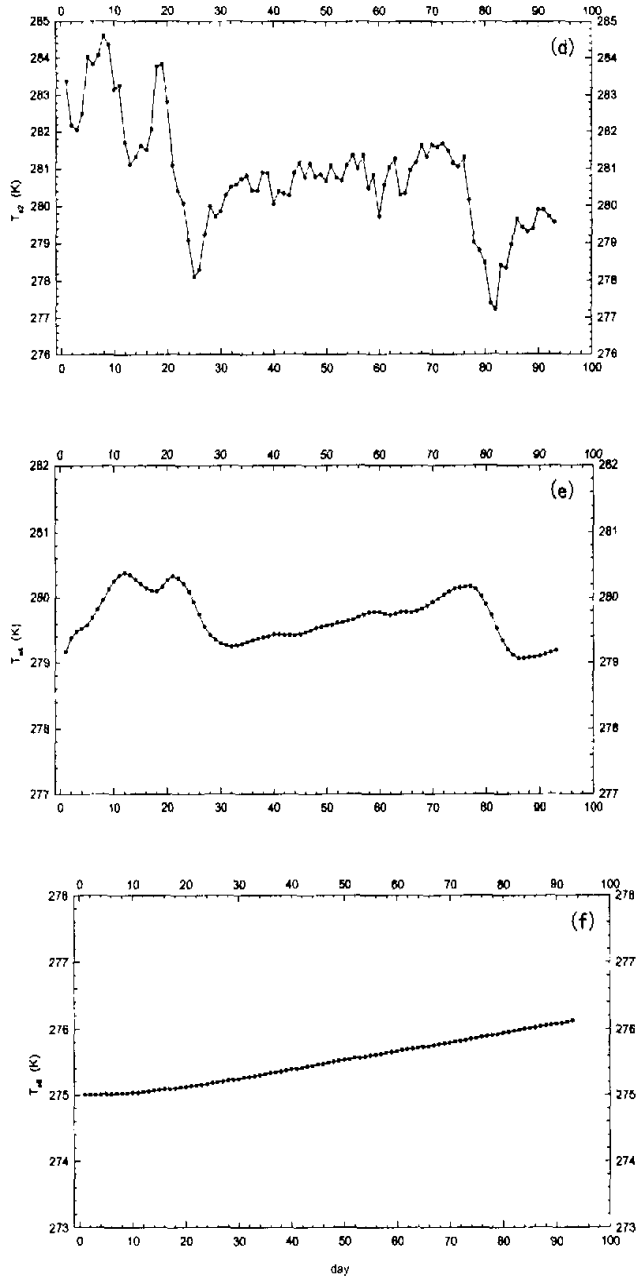

Fig. 5. Same as Fig. 5(a,b,c) but for soil temperature (T_s) at 2nd (d), 4th (e), and 6th (f) layer (in depth of 0.2 m, 1.1 m and 4.7 m respectively).

(Fig. 6). The responses of T_s at different levels lag one by one as depth increases with weakening amplitude. For example, T_s in layer six (T_{s6}, and hereafter) lags T_{s2} by 2 months and

its amplitude is only 1 / 6 of T_{s2}, which agrees well with observations (Guo 2000).

Table 4. Same as Table 3 but the forced heat flux at soil bottom in SR3 is 10 W m^{-2}

	ΔF_{GEV} (W m^{-2})	ΔF_{GR} (W m^{-2})	ΔF_{SH} (W m^{-2})	ΔT_g (K)	ΔT_{s1} (K)	ΔT_{s2} (K)	ΔT_{s3} (K)	ΔT_{s4} (K)	ΔT_{s5} (K)	ΔT_{s6} (K)
01–10	0.43	13.43	−11.5	−0.61	−0.46	−0.21	0.11	0.81	1.59	1.00
11–20	1.28	4.85	−4.90	−0.33	−0.11	0.20	0.51	1.18	3.13	3.17
21–30	0.91	−4.10	2.07	0.51	0.47	0.31	0.20	0.70	3.06	5.14
31–40	−0.44	0.27	0.01	0.22	0.34	0.63	1.03	1.56	2.90	6.64
41–50	−0.30	−1.27	1.15	0.15	0.22	0.55	1.05	1.75	3.33	7.87
51–60	1.49	−3.88	1.61	0.24	0.29	0.52	1.04	1.95	3.73	8.93
61–70	0.53	−2.20	0.68	0.36	0.46	0.71	1.20	2.02	3.97	9.84
71–80	4.75	−9.66	3.91	0.42	0.44	0.46	0.80	1.96	4.33	10.6
81–93	1.90	−6.55	2.37	0.81	0.93	1.08	1.29	1.75	3.85	11.2

The comparison between the results of CR and SR1 (Table 2) shows that the largest difference is ΔT_{s6} =6.51°C for deep layer soil temperature in last time period. Since the soil conductive process prevents the anomaly from spreading upwards, ΔT_{s5} declines sharply to 1.26°C and ΔT_{s1} is only 0.08°C. Accordingly, no change of T_g can be identified until day 30. ΔT_g is only 0.06°C in last time segment. No increase greater than 1 W m^{-2} can be found in sensible (ΔF_{SH}) and ground heat fluxes (ΔF_{GR}).

However, distinct differences appear in SR2 (Table 3). All these changes can be reasonably ascribed to the increase of soil thermal conductivity. Higher conductivity results in faster heat exchange in a multi–layer soil. As a matter of fact, enlarging of thermal conductivity is a substitution of convective heat transfer for the sake of simplicity because convection is more efficient than conductivity in transferring heat. As a result, anomalies of T_s at all levels were reduced in much degree although the total amount of introduced heat into the soil is same as that in SR1. Being affected by the surface heat balance and underground soil heat flux simultaneously, T_g seems more changeable than other variables. Its value in SR2 during starting 20 days was even less than that in CR. But remarkable positive anomaly appeared since the 3rd time segment resulted from the contribution of the forced heat flux. Increase in T_g was 0.65°C in last period. It is larger than the anomaly in SR1 by 10 times! The results are consistent with the idea in section 1.2 that convection is more efficient than conduction in affecting land surface energy budget.

A little bit more extreme condition is considered in SR3 by enhancing the heat flux into the bottom of the soil layer to 10 W m^{-2}. From Table 4, notable increase in soil temperature at the deepest layer (T_{s6}) of 1°C is already detected in the first 10 days (Table 4). Such a strong forcing finally resulted in a anomaly of 11.2°C. Also, increase in T_g reaches 0.81°C eventually due to persistent heating. As for the heat flux into land surface (F_{GR}), the net gaining throughout the whole period is 20 W m^{-2} or so (negative into surface). Comparison on the rest variables can refer to Table 2, Table 3, and Table 4 and will not be treated here.

4. Conclusions and discussions

Statistical relationship between soil thermal anomaly and short–term climate change (precipitation change in particular) is presented in this paper based on a typical case. The

possible physical mechanism and soil thermal effects on T_s, T_g, and surface energy budget as well as the associated physical processes are then investigated using an off-line land surface model by taking underground heat flux into consideration. Although it is a quite preliminary work, some results are meaningful.

The results show that the soil thermal effects on surface energy balance may be improperly treated in current land surface models. The reason for such disposal is that the "hot fluid" convection process associated with the heat release in soil was not included in the models while it may deserve more attention. The idea is demonstrated both in data analyses and numerical modeling ways. Studies by Wang (1991) show that notable increase in precipitation, air temperature, and humidity as well as the decrease in surface level pressure can be expected due to a anomaly of 1°C in T_g for 30 days. Based on the results mentioned above, we may have following viewpoint: emission of some 'hot fluid' (such as CO_2 and water vapor etc.) from deep soil layer on a certain spatial-temporal scale would give an important influence on soil temperature, especially on ground temperature. As a result, increase in sensible / latent heat flux and outgoing long-wave radiation on land surface eventually will cause the short-term climate change.

It should be pointed out that there is much room left for improvement of this problem due to the complexity and uncertainty of climate change. Among them are: more attention should be paid to get the regional spatial / temporal characteristics of soil thermal anomaly, soil wetness and hydrologic processes, which are closely related to soil temperature change, were not mentioned in this paper. In addition, integration for longer period and using coupled land-atmosphere model are also helpful for better understanding of this issue.

The authors would like to thank Dr. Zhang Yu for providing intensified atmospheric boundary layer data during GAME Tibet and we highly appreciate the contributions made by all the members in field experiment.

This paper is jointly sponsored by China NKBRSF Project G1999043400, National Natural Science Foundation of China under Grant Nos.49835010 and 40075019, and China Post Doctoral Science Foundation.

REFERENCES

Bonan, G. B., 1995a: Land-atmospheric CO_2 exchanges simulated by a land surface process model coupled to an atmospheric general circulation model. *J. Geophys. Res.*, **100D**, 2817-2831.

Bonan, G. B., 1995b: Land-atmosphere interactions for climate system models: coupling biophysical, biogeochemical, and ecosystem dynamical processes. *Remote Sens. Environ.*, **51**, 57-73.

Bonan, G. B., 1996 The NCAR Land Surface Model (LSM version 1.0) coupled to the NCAR Community Climate Model. *NCAR Technical Note NCAR/ TN-429+STR*, National Center for Atmospheric Research, Boulder, Colorado.

Dickinson, R. E., A. Henderson-Sellers, and P. J. Kennedy, 1993: Biosphere-Atmosphere Transfer Scheme (BATS) VERSION 1e as coupled to the NCAR Community Climate Model. NCAR Technical Note NCAR TN-387+STR, National Center for Atmospheric Research, Boulder, CO.

Etiope, G., and R. W. Klusman, 1998: Does geogas emission in non-volcanic areas contribute to carbon cycle and global climate change? *Proceedings of the 25th I.S.Q.E. Course " OBSERVATIONAL DATABASE AND MECHANISMS OF CLIMATE"*, Erice-Sicily, Italy, 21-27 Nov. 1998.

Guo, W. D., 2000 Impacts of soil temperature field on precipitation field both in statistic and numerical ways. Dissertation of Lanzhou Institute of Plateau Atmospheric Physics, Chinese Academy of Sciences.

Shangguan, Z. G. et al., 2000: Characteristics of magma gas emission originated from mantle in geothermal regions of Tenchong, Yunnan Province. *Science in China (Ser. D)*, **30**, 407-414 (in Chinese).

Tang, M. C., and X. Q. Gao, 1997a. Some statistical characteristics of geothermal vortex in China during 1980-1993 (I). *Science in China (Ser.D)*, **40**, 561-568.

Tang, M. C., and X. Q. Gao, 1997b: Some statistical characteristics of geothermal vortex in China during 1980–1993 (II). *Science in China* (*Ser. D*), **40**, 569–576.

Tang, M. C. et al., 1998: Evidences for "great gorge" of Brahmaputra as a "hot spot" on the earth. *Science in China* (*Ser. D*), **28**, 463–468 (in Chinese).

Wang, W. Q., 1991: Numerical simulation of the impacts of soil temperature / wetness on short-term climate change. *Chinese Journal of Atmospheric Sciences*, **15**, 115–123.

Yuan, D. X., 1999: Progress in the study on Karst processes and carbon cycle. *Advances in Earth Sciences*, **14**, 425–432 (in Chinese).

Zhao, Z. G., 1998: Advances in precipitation prediction during flood season in China. *Remarks on climate prediction* (*internal publication of National Climate Center*), 91–98 (in Chinese).

土壤热异常影响地表能量平衡的个例分析和数值模拟

郭维栋　孙菽芬　钱永甫

P4 A

摘　要

首先给出了土壤热异常与短期气候变化的一个典型个例，进而基于一个 off-line 的陆面过程模式，通过改变进入土壤底层的热强迫，讨论了土壤热异常影响地表能量平衡过程可能的物理机制。

在实验Ⅰ中，在土壤底层(6.3 m)引入 5 W m^{-2} 的热通量积分 3 个月，发现与控制试验(土壤底部为零通量，即无热量的流入／流出)相比，地表仅有 0.06℃的增温。实验Ⅱ在Ⅰ的基础上将土壤热传导系数放大一个等级以加速土壤中的热交换过程，发现地表增温可达 0.65℃。若再将热强迫增至 10 W m^{-2}，则地表增温可达 0.81℃，且地表感热通量的增幅可达约 10 W m^{-2}，这对短期气候变化已不可忽视。结果表明：当土壤热异常达到一定强度并且能较快上传时将对地表能量平衡过程产生明显影响。因此目前陆面过程模式中普遍忽略来自深部土壤热流的做法值得商榷。同时，客观地表述深部热流体在土壤中的传输过程及应用陆气耦合模式对深入理解这一问题也是必要的。

关键词：土壤热异常，陆面过程模式，地表能量平衡